Research Square

Preprints are preliminary reports that have not undergone peer review.
They should not be considered conclusive, used to inform clinical practice,
or referenced by the media as validated information.

Ginsenoside C3 alleviates myocardial ischemia/reperfusion injury by inhibiting TRPM7 and activating the Nrf2-Keap1-HO-1 signaling pathway

Ziyuan Wang
China Three Gorges University
Zhiwen Zhou
China Three Gorges University
Ruiyi Luo
China Three Gorges University
Yongkang Peng
China Three Gorges University
Caili Zhang
China Three Gorges University
Qiong Du
China Three Gorges University
Shizhong Zhang
zhangsz@ctgu.edu.cn
China Three Gorges University

Article

Keywords: Myocardial ischemia reperfusion injury, Ginsenoside derivatives, Apoptosis, Oxidative stress, TRPM7, Nrf2

Posted Date: November 6th, 2026

DOI: https://doi.org/10.21203/rs.3.rs-10810137/v1

License: This work is licensed under a Creative Commons Attribution 4.0 International License.
Read Full License

Additional Declarations: No competing interests reported.

Ginsenoside C3 alleviates myocardial ischemia/reperfusion injury by inhibiting TRPM7 and activating the Nrf2-Keap1-HO-1 signaling pathway

Ziyuan Wang[1], Zhiwen Zhou[3], Ruiyi Luo[1],Yongkang Peng[1], Caili Zhang[1] Qiong Du[2#], Shizhong Zhang[1#]

1 Hubei Key Laboratory of Tumor Microenvironment and Immunotherapy, Basic medical College of China Three Gorges University, Yichang 443002, China;

2 Department of Neurology, Yiling People's Hospital of Yichang, Yichang 443002, China

3 Department of Pharmacy, Medical College， China Three Gorges University, Yichang 443002, China

Corresponding authors：

Professor Shizhong Zhang: E-mail: zhangsz@ctgu.edu.cn; Address: Daxue Road 8, College of Basic Medical Sciences of China Three Gorges University, Yichang, 443002.

Dr Qiong Du: E-mail: 243244811@qq.com;

Abstract

Aims: Ginsenosides are major bioactive components of ginseng and have been demonstrated to provide protective activity against injury triggered by myocardial ischemia/reperfusion (MIRI). Drawing on the structural attributes of naturally occurring ginsenosides, we synthesized a novel ginsenoside derivative, Compound 3 (C3). This investigation aimed to evaluate the protective effects of C3 against MIRI and to clarify the molecular mechanism underlying its action.

Materials and methods: In vivo and ex vivo rat MIRI models were established. Both models were subjected to 30 min ischemia followed by reperfusion. Cardiac functional indices, including LVDP, LVEDP, and ±dp/dtmax, were recorded to evaluate cardiac function. Myocardial infarct size, LDH activity, MDA levels, and SOD activity was

measured to assess myocardial damage and oxidative stress. HE staining enabled observation of myocardial morphological changes. Cardiomyocyte apoptosis was detected via TUNEL assay. Finally, Western blot quantified protein expression of TRPM7, Bax, Bcl-2, Cleaved-Caspase3, Keap1, Nrf2, HO-1.

Results: In MIRI models, C3 treatment significantly restored impaired cardiac function, reduced histopathological injury, and suppressed oxidative stress. C3 markedly inhibited TRPM7 expression, promoted activation of the Nrf2-Keap1-HO-1 antioxidant pathway, and lessened apoptosis in cardiomyocytes. The TRPM7 inhibitor NS8593 recapitulated the cardioprotective effects of C3, whereas the TRPM7 agonist MIB abrogated C3-mediated protection.

Significance: This study demonstrates that the novel ginsenoside derivative C3 alleviates MIRI via attenuation of oxidative stress and decreased cardiomyocyte apoptosis. Mechanistically, C3 inhibits TRPM7, which in turn promotes activation of the downstream Nrf2–Keap1–HO-1 cascade. These findings offer preclinical evidence that C3 represents a promising agent for MIRI therapy.

Keywords: Myocardial ischemia reperfusion injury; Ginsenoside derivatives; Apoptosis; Oxidative stress; TRPM7 ; Nrf2

1.Introduction

Ischemic heart disease (IHD) ranks among the leading global causes of death, with its mortality rate steadily increasing worldwide[1]. IHD refers to the pathophysiological phenomenon in which damage to myocardial tissue is further exacerbated following the recanalization of partially or fully occluded coronary arteries[2]. At present, thrombolysis and percutaneous coronary intervention (PCI) remain the most broadly employed and efficacious strategies for diminishing infarct size, preserve left ventricular systolic performance, and reducing susceptibility to heart failure[3]. Although these interventions can rapidly relieve ischemic damage, restoring perfusion nevertheless triggers a chain of detrimental pathological responses, including excessive reactive oxygen species (ROS), intracellular Ca^{2+} overload, and inflammatory activation, which further exacerbate cardiac dysfunction and ultimately trigger extensive cardiomyocyte death. This pathological cascade is defined as myocardial

ischemia/reperfusion injury (MIRI)[4-6]. Despite substantial advances in cardioprotective research, clinically viable interventions to alleviate MIRI are still absent. Despite substantial advances in cardioprotective research, clinically viable interventions to alleviate MIRI are still absent. Accordingly, it is critical to clarify the pathogenic mechanisms underlying MIRI, so as to discover promising therapeutic targets for IHD and its secondary myocardial damage.

Ginsenosides are important bioactive triterpenoid saponins isolated from ginseng. According to the skeleton structure of the ginsenoside aglycone, they are classified into three main types: dammarane, oleanolic, and octotillol. Within the dammarane category, two subtypes are recognized, namely PPD (protopanaxadiol) and PPT (protopanaxatriol)[7]. Aglycones in the PPD class include Rg3, Ra1, Ra3, Ra2, and Rh2; by contrast, the PPT category comprises F1, Rg1, Rg2, and Rf [8]. Cumulative evidence demonstrates that ginsenosides exert prominent protective effects against MIRI[9]. Among these ginsenosides, the aglycones Rg3 and Rh2 exhibit anti-inflammatory, antioxidative and anti-MIRI bioactivities[10, 11].

Nevertheless, research focusing on structural modification and pharmacological evaluation of ginsenoside aglycones was previously constrained by their low natural abundance and high purification costs. In recent years, advances in separation and chemical synthesis techniques for ginsenosides, coupled with growing demand to enhance oral bioavailability, have driven extensive research into novel semi-synthetic ginsenoside derivatives[12]. Our research group previously synthesized Compound 3 (C3), a novel ginsenoside derivative that integrates the shared aglycone scaffold of both Rg3 and Rh2. To date, no published studies have clarified whether C3 recapitulates the anti-inflammatory and antioxidant capacities of natural ginsenosides, or whether it confers therapeutic benefits against MIRI.

The TRP (transient receptor potential) channel family constitutes a superfamily of non-voltage-gated cation channels, which was, initially identified in Drosophila melanogaster by Cosens et al. in 1969[13] Up to now, 28 genes encoding subunits of TRP channels have been recognized. The TRP superfamily is further classified into seven subgroups, namely TRPA, TRPC, TRPM, TRPML, TRPN, TRPP, and TRPV [14].

Within the TRPM subfamily, TRPM7 (transient receptor potential cation channel subfamily melastatin 7) displays a distinctive bifunctional organization, comprising an ion-permeable pore alongside a serine/threonine kinase domain[15]. TRPM7 is broadly distributed across cardiac, cerebral, pulmonary, and renal tissues, as well as various other organs and tissues, and is involved in various physiological events including cellular development and ion homeostasis[16, 17]. Accumulating evidence demonstrates that pharmacological blockade of TRPM7 mitigates ischemia/reperfusion-induced tissue damage and reduce ROS generation [18]. Nevertheless, no existing literature has clarified whether C3 exerts protective effects against MIRI via TRPM7 suppression.

Oxidative stress represents a primary driver of MIRI[19]. Nuclear factor erythrocyte-derived factor 2 (Nrf2) exerts antioxidant cardio protection by upregulating a panel of antioxidant proteins [20]. Kelch-like ECH-associated protein 1 (Keap1) is an endogenous chaperone essential for maintaining cellular redox homeostasis [21]. Under normal physiological conditions, cytoplasmic Nrf2 binds to Keap1 and undergoes ubiquitin-mediated proteasomal degradation, which silences its transcriptional activity in the nucleus; however, during oxidative stress triggers conformational rearrangement of Keap1 and thereby blocks Nrf2 degradation[22]. Stabilized Nrf2 translocate into the nucleus, binds to antioxidant response element, and initiates the transcription of the downstream antioxidant gene HO-1. This cascade suppresses myocardial ROS accumulation and reinforces intrinsic antioxidant defense[23]. Cumulative evidence demonstrates that ginsenoside Rg3 activates the Nrf2-Keap1 axis to reduce the area of myocardial infarction and boost cellular antioxidant capacity[21]. Collectively, , we hypothesized that C3 elicits cardio protection through modulation of the Nrf2-Keap1-HO-1 signaling cascade; however, no prior study has clarified the functional link between C3, TRPM7 and the Nrf2 pathway in the setting of MIRI.

Apoptosis represents the predominant mode of cardiomyocyte death during MIRI, and the mitochondrial intrinsic apoptotic cascade is mainly governed by the pro-apoptotic protein Bax and anti-apoptotic Bcl-2[24]. Apoptotic stimuli break the homeostatic balance between Bcl-2 and Bax, which triggers cytochrome C (Cyt-C) release., Cyt-C subsequently activates caspase-3, ultimately triggering the full apoptotic

program[25, 26]. Suppression of cardiomyocyte apoptosis is critical for preserving cardiac function and improving patient prognosis after MIRI[27]. Nevertheless, it remains unclarified whether C3 modulates apoptosis in injured cardiomyocytes via TRPM7 inhibition.

On the basis of the above literature evidence, we proposed the hypothesis that the novel ginsenoside derivative C3 suppresses TRPM7 to activate the Nrf2-Keap1-HO-1 antioxidant cascade, thereby exerting anti-oxidative and anti-apoptotic activities and alleviating MIRI. In the present work, ex vivo isolated heart and in vivo rat MIRI models were constructed to separately evaluate C3's effects at the organ level and within intact systemic physiological environments, as well as to dissect its underlying molecular mechanisms. Collectively, our experimental observations offer fundamental preclinical evidence and lay a theoretical foundation for developing targeted therapeutic interventions against MIRI.

2.Materials and methods

2.1. Animal

All procedures involving animals were carried out in compliance with the NIH (National Institutes of Health) guidelines on animal care and use, and the study protocol was approved by China Three Gorges University's ethics committee for laboratory animal care. Male Sprague-Dawley rats, six weeks of age, were supplied by the Animal Experimentation Center of China Three Gorges University. They were kept at standard room temperature on a 12 h light/12 h dark cycle and allowed unrestricted access to regular rodent chow and water. humidity was maintained between 55% and 65%. The animal care license number is SYXK (E) 2017-0061.

2.2. Structure and synthesis of ginsenoside derivative 3

Figure 1 depicts the synthetic pathway leading to triterpenoid derivative 3. At

the outset, the 3,12-dihydroxy moieties of PPD were masked as a diacetate with DMAP and acetic anhydride, yielding compound 1. Reaction of 1 with *m*-CPBA afforded epoxide 2, which was subsequently treated with Jones reagent to give acetylated lactone 3. Subsequent base-mediated deprotection and acidification provided lactone 4 in acceptable yields. Next, Compound 4 undergoes successive aminolysis and esterification to give compound 3.

PPD (500 mg, 1.08 mmol) and DMAP (20 mg, 0.16 mmol) were dissolved within anhydrous pyridine (4 mL). Dropwise addition of acetic anhydride (0.42 mL, 4.43 mmol) was performed, and followed by 24 h agitation under ambient temperature conditions. Ethyl acetate diluted the crude mixture, which was consecutively rinsed by 10% HCl, purified water and saturated brine. After drying over anhydrous sodium sulfate and vacuum concentration, crude residue was purified on silica-gel columns (petroleum ether-ethyl acetate =10:1) to obtain white solid 3β,12β-O-diacetyl-20(S)-protopanaxadiol (**1**) (515 mg, 86%).

Substrate **1** (208 mg; 0.38 mmol) was taken up in dichloromethane (10 mL), and the resulting solution was chilled to 0°C. After the mixture had been cooled, a dichloromethane solution (10 mL) containing m-CPBA (0.76 mmol; 185 mg; 75%) was introduced in a dropwise fashion, and stirring was maintained for 2 h. The organic phase was then washed sequentially with saturated aqueous $NaHCO_3$, saturated aqueous $Na_2S_2O_3$, H_2O, and brine, and dried over Na_2SO_4. After concentration under reduced pressure, the crude material was purified by silica-gel column chromatography, eluting with petroleum ether/EtOAc (8:1). The title compound (20S,24)-epoxy-3β,12β-O-diacetyl dammarane-25-ol (2) was isolated as a white powder (145 mg, 69%).

Compound **2** (370 mg, 0.66 mmol) was dissolved in acetone (10 mL), after which Jones reagent (4 mL) was introduced. The resulting mixture was stirred at ambient temperature for 4 h. Acetone was evaporated in vacuo, and ethyl acetate (100 mL) was then added. The organic phase was washed successively with H_2O and brine, dried with Na_2SO_4, and concentrated. The crude residue was subjected to silica gel column chromatography, eluting with petroleum ether-ethyl acetate (6:1). This gave (20S,24)-Epoxy-3β,12β-O-diacetyl-24-carbonyl dammarane (**3**), which was obtained as a white

powder (300 mg, 89%).

Compound **3** (0.59 mmol; 305 mg) was dissolved in a mixed solvent of methanol and H_2O (15 mL/3 mL), and potassium hydroxide (1.18 mmol; 66 mg) was then added. The resulting solution was heated at reflux for 3 h. After cooling, the pH was brought to 1 by addition of aqueous sulfuric acid (50%). The mixture was then maintained at 60°C with stirring for 2 h. Methanol was evaporated in vacuo, and the remaining material was diluted with dichloromethane. The organic layer was washed with H_2O and brine, dried over Na_2SO_4, and concentrated. The crude product was purified by column chromatography on silica gel using petroleum ether-ethyl acetate (1:1). This afforded (20S,24)-Epoxy-24-carbonyl dammarane-3β,12β-diol (**4**) as a white solid in 90% yield (230 mg)[28].

A THF (8 mL) solution containing compound **4** (62 mg, 0.15 mmol) was treated with sodium hydroxide (10 mg, 0.25 mmol) and the amine (0.30 mmol). The resulting mixture was stirred at ambient temperature for 8 h, after which the volatiles were removed in vacuo. The residue was taken up in ethyl acetate, and the organic layer was washed sequentially with H_2O and brine, dried over Na_2SO_4, filtered, and concentrated. The crude material was purified by silica-gel column chromatography, eluting with a petroleum ether-ethyl acetate (4:1 to 1:1), to provide the target compound **5**[29].

Heptanoic acid (0.36 mL, 3.78 mmol) was introduced at ambient temperature into a dry pyridine (10 mL) solution of compound 5 (600 mg, 1.26 mmol) and DMAP (24 mg, 0.19 mmol) with stirring. After 12 h, the reaction mixture was diluted with EtOAc. The resulting solution was washed in sequence with 10% HCl, H_2O, and the brine. The organic layer was dried over Na_2SO_4 and concentrated evaporated. The crude product was purified by silica-gel column chromatography (petroleum ether-EtOAc, 8:1) to afford **6** as a white-colored solid.

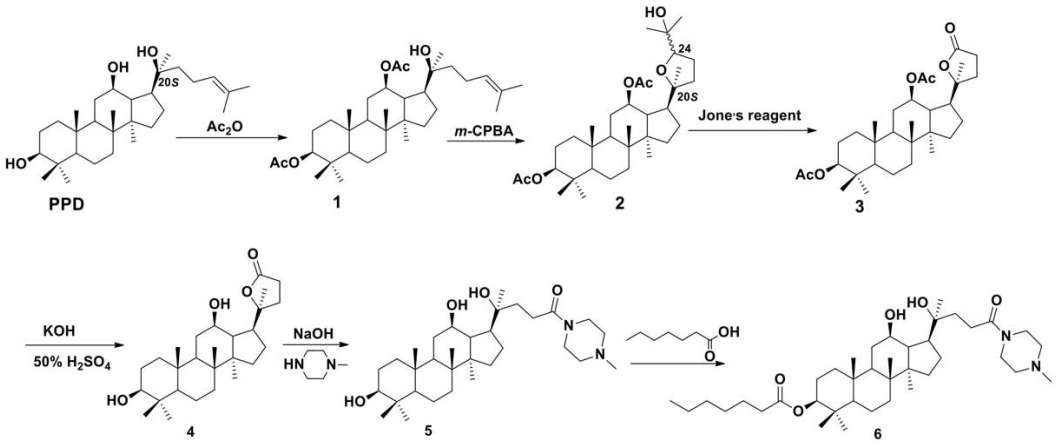


Figure 1. Synthesis process of ginsenoside derivative 3

2.3. Ex vivo myocardial ischemia-reperfusion model

An ex vivo myocardial ischemia-reperfusion model was primarily established using a Langendorff perfusion apparatus. Rats were first anesthetized with sodium pentobarbital (50 mg/kg) and then decapitated. The heart was removed and placed in pre-chilled, oxygenated Krebs-Henseleit's solution (K-H buffer). The heart was immediately transferred to and secured in a Langendorff perfusion apparatus. A pre-prepared water-filled latex balloon was inserted through the incised left atrial appendage into the left ventricle; perfusion was initiated immediately after fixation. The perfusion fluid pressure was maintained at a constant 80 mmHg at 37°C; the fluid was pre-oxygenated with 95% O_2 and 5% CO_2 for 30 min, and the pH was maintained between 7.35 and 7.45. Data including left ventricular diastolic pressure (LVDP), left ventricular end-diastolic pressure (LVEDP), and the maximum rate of change of left ventricular pressure (±dp/dtmax) were recorded using the TM-Wave pressure transduction software (ADInstruments Ltd., Australia). Experimental procedures were performed after each group of hearts had completed perfusion equilibration for at least 20 min to reach a stable state. The rats were randomly divided into eight groups, with six rats in each group: Sham group, Ischemia/Reperfusion (I/R) group, C3 group (0.1 μmol/L, 0.01 μmol/L, 0.001 μmol/L), NS8593 group (TRPM7 inhibitor NS8593, Medchemexpress, HY-137952), MIB group (Mibefradil, a TRPM7 agonist,

Medchemexpress, HY-15553A), and MIB+C3 group. Hearts in the Sham group were perfused continuously with K-H solution for 150 min; hearts in the I/R group, C3 group, NS8593 group, MIB group, and MIB+C3 group were all subjected to 30 min of ischemia. For all drug concentrations, 20 min of reperfusion with K-H solution containing the respective drug concentration was initiated 30 min after ischemia, followed by perfusion with K-H solution; The NS8593 group was perfused with K-H solution containing NS8593 (0.75 μmol/L[30]) for the first 20 min, followed by reperfusion with K-H solution; The MIB group was perfused with K-H solution containing MIB (70 μmol/L[15]) for the first 20 min, followed by reperfusion with K-H solution; The MIB+ drug group was perfused with K-H solution containing MIB (70 μmol/L) for the first 20 min; following ischemia, the group was perfused with K-H solution containing the drug (0.1 μmol/L) for 20 min, followed by perfusion with K-H solution (Fig 2A).

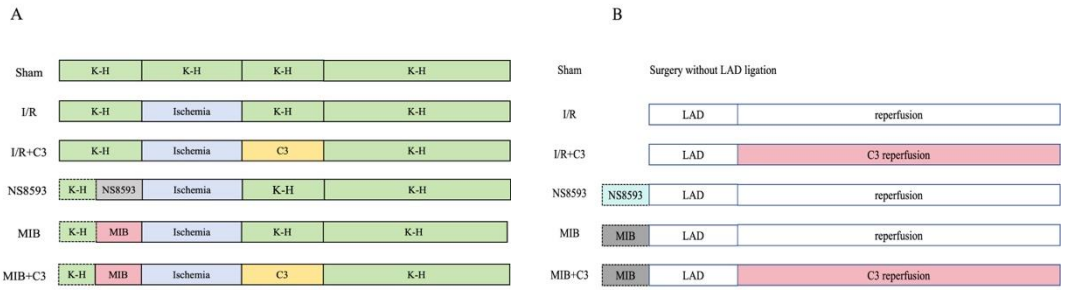


Figure 2. Schematic diagram of the MIRI model experimental protocol. (A) Ex vivo MIRI model. (B) In vivo MIRI model

2.4. In vivo myocardial ischemia-reperfusion model

In vivo model of myocardial ischemia-reperfusion was primarily established by ligating the left anterior descending artery (LAD). Rats were subjected to a 12 - hour fasting period before surgical operation. After intraperitoneal anesthesia with sodium pentobarbital (50 mg/kg), the chest was opened via thoracotomy, and the LAD was ligated using 5-0 silk suture. A significant ST-segment elevation detected by limb-lead ECG (Opto-Electronics Corp., Japan) served as the indicator of successful LAD

ligation and myocardial ischemia. After 30 min of ischemia, the ligature was loosened to restore perfusion, followed by 120 min reperfusion. Rats were randomly divided into eight groups (n=6 per group): the sham group (Sham), the ischemia/reperfusion group (I/R), the C3 group (0.2 mg/kg, 0.5 mg/kg, 1.0 mg/kg), the NS8593 group, the MIB group, and the MIB+C3 group. The Sham group received identical thoracotomy without LAD ligation, whereas all other groups were subjected to LAD occlusion. For C3 subgroups , 1 mL of C3 solution (0.5 mg/kg) was injected via femoral vein at the onset of reperfusion; For the NS8593 group, 1 mL of NS8593 solution was administered into the femoral vein prior to surgery (2 mg/kg [31]). For the MIB group, 1 mL of MIB solution (3 mg/kg) was injected into the femoral vein prior to surgery. For the MIB+C3 group, 1 mL of MIB solution (3 mg/kg) was injected into the femoral vein prior to surgery, followed by injection of 1 mL of C3 solution (0.5 mg/kg) via the same vein immediately after 30 min ischemia. All cardiac tissues were harvested for subsequent detection after reperfusion (Figure 2B).

2.5. Lactate dehydrogenase (LDH) measurement

For the ex vivo myocardial ischemia/reperfusion model: Coronary effluent was collected at five time points: at the end of equilibration, as well as at 5, 10, 15, and 30 min after reperfusion. The optical density (OD) values of effluent samples were detected using a LDH assay kit (Nanjing Jiancheng Biotechnology Corp., Ltd.) via spectrophotometry, and LDH activity was calculated accordingly.

For the in vivo myocardial ischemia/reperfusion model, abdominal aortic blood was collected after model establishment, and serum was isolated for detection. Similarly, the OD values were measured by spectrophotometry with the same LDH assay kit, and serum LDH activity was calculated.

2.6. Measurement of superoxide dismutase (SOD)and malondialdehyde (MDA)

For the ex vivo myocardial ischemia/reperfusion model, 100 mg of myocardial

tissue was homogenized in 0.9% saline solution. After centrifugation, the supernatant was harvested. Myocardial MDA and SOD levels were detected using commercial assay kits (Nanjing Jiancheng Biotechnology Corp., Ltd.) according to the manufacturer’s instructions. Total protein concentration was quantified via the BCA method (P1511-3; Prilay Corp., China).

For the in vivo model, blood samples were collected from the abdominal aorta after model establishment. Serum was isolated by centrifugation and used for the detection of MDA and SOD levels with the same assay kits.

2.7. 2,3,5-Triphenyl-2H-Tetrazolium Chloride (TTC) staining

After modeling, myocardial samples were harvested, embedded in embedding medium (G6059-110ML; Servicebio, China), and frozen at −20° C for 40 min. Subsequently, the frozen tissues were cut into approximately 2 mm thick transverse sections and incubated with TTC staining solution (G1017-100ML; Servicebio, China) at 37° C for 10 min. Stained sections were fixed in 4% paraformaldehyde (G1101-500ML; Servicebio, China) for 40 min. ImageJ software (National Institutes of Health, Bethesda, MD, USA) was applied to quantify the infarct area and the area at risk (AAR). In TTC staining, white regions indicate infarcted myocardium, while red regions represent viable myocardium at risk. The myocardial infarct size was calculated and presented as the percentage of infarct area relative to the total area at risk.

2.8. Hematoxylin and eosin (HE) staining

Cardiac specimens collected after the procedure were washed in physiological saline and subsequently immersed in 4% paraformaldehyde for overnight fixation. The fixed material was then embedded in paraffin and sectioned at a nominal thickness of 4 μm. The paraffin sections were dewaxed twice in xylene (Sinopharm Reagent Corp., Ltd., China), 25 min per wash, followed by hematoxylin-eosin (HE) staining (G1004-100ML; Servicebio, China). After the staining procedure, the sections were dehydrated

through a graded ethanol series, clarified in xylene, and ultimately mounted with neutral balsam. Histological images were captured under an Olympus light microscope.

2.9. TUNEL staining

Prepared hearts were washed with physiological saline, after which the specimens underwent overnight fixation in 4% paraformaldehyde. The fixed material was then embedded in paraffin and cut into sections of about 4 μm thickness. The paraffin sections were subsequently deparaffinized twice in xylene for 25 min per wash. TUNEL labeling was conducted according to the protocol provided with a one-step TUNEL apoptosis assay kit from Biyuntian Biotechnology Corporation. Afterward, the sections were counterstained at room temperature using 4',6-diamidino-2-phenylindole (DAPI; Biyuntian Biotechnology Corp., Ltd.). They were then mounted with an anti-fade mounting reagent and examined by fluorescence microscopy to determine the number of apoptotic cardiomyocytes.

2.10. Western blot analysis

Cardiac tissues (about 50 mg) were weighed, cut into small pieces, and placed in a centrifuge tube. Total protein was extracted by adding prepared RIPA lysis buffer (Servicebio, China; G2002). Each sample's protein content was determined using the BCA assay. Equivalent protein quantities were loaded and resolved by polyacrylamide gel electrophoresis in the presence of sodium dodecyl sulfate (SDS-PAGE). The resolved proteins were then transferred electrophoretically to PVDF (polyvinylidene fluoride) membranes (Millipore, USA), followed by blocking with 5% skimmed milk for at least 90 min.

The membranes were subjected to overnight incubation at 4 °C with primary antibodies targeting the proteins listed below: TRPM7 (1:500; 55251-1-AP; Proteintech, China), NRF2/NFE2L2 (1:2000; 16396–1-AP; Proteintech, China), KEAP1 (1:2000; 10503–2-AP; Proteintech, China), HO-1/HMOX1 (1:5000; 10701–1-AP; Proteintech, China), BAX (1:20,000; 50599-2-Ig; Proteintech, China), BCL2 (1:2000; 12789-1-AP; Proteintech, China), Cleaved Caspase-3 (1:500; 25128-1-AP; Proteintech, China), and

β-actin (1:10,000; 20536-1-AP; Proteintech, China). Following washing, the blots were exposed to a horseradish peroxidase-linked secondary antibody generated in goat against rabbit IgG (H+L) (1:10,000; GB23303; Servicebio, China) for 1h at ambient temperature. Bands were then developed using an ECL reagent (G2020-50ML; Servicebio, China) and recorded with a chemiluminescence imaging platform. Band gray intensities were finally quantified with ImageJ software.

2.11. Statistical analysis

Values were shown as the mean with standard deviation (SD), based on a minimum of three separate biological replicates. GraphPad Prism 10 was employed for statistical evaluation. Unpaired t-tests were used for two-group comparisons, whereas a one-way analysis of variance, abbreviated as ANOVA, was utilized when more than two groups were compared. A threshold of $P < 0.05$ was regarded as statistically significant. Significance is denoted by asterisks in the following manner: $^{*}P < 0.05$, $^{**}P < 0.01$, $^{***}P < 0.001$, $^{****}P < 0.001$.

3. Result

3.1. C3 improved cardiac contractile function and alleviated myocardial infarct size in ex vivo MIRI hearts

Hemodynamic indices were detected using the ex vivo MIRI model. Compared with the Sham group, the I/R group exhibited markedly lower LVDP (Figure 3A), +dp/dtmax (Figure 3C), and -dp/dtmax (Figure 3D) as well as elevated LVEDP (Figure 3B) at 5, 10, 15, and 30 min after reperfusion. Treatment with graded concentrations of C3 reversed these abnormalities: LVDP, +dp/dtmax and -dp/dtmax at all detected time points were notably higher, accompanied by a decline in LVEDP relative to the I/R group (Figure 3A – D).

Notably, 0.1 μmol/L C3 exerted the strongest protective effect on cardiac systolic and diastolic function at 5 min post-reperfusion; thus, this concentration was adopted for all subsequent mechanistic experiments (Figure 3E–H).

We further quantified myocardial infarct area to verify the cardioprotective

capacity of C3. Larger infarct size was observed in the I/R group (Figure 3I, J). All C3 intervention groups displayed varying degrees of infarct reduction, among which 0.1 μmol/L C3 yielded the most remarkable infarct-limiting effect. (Figure 3I, J).

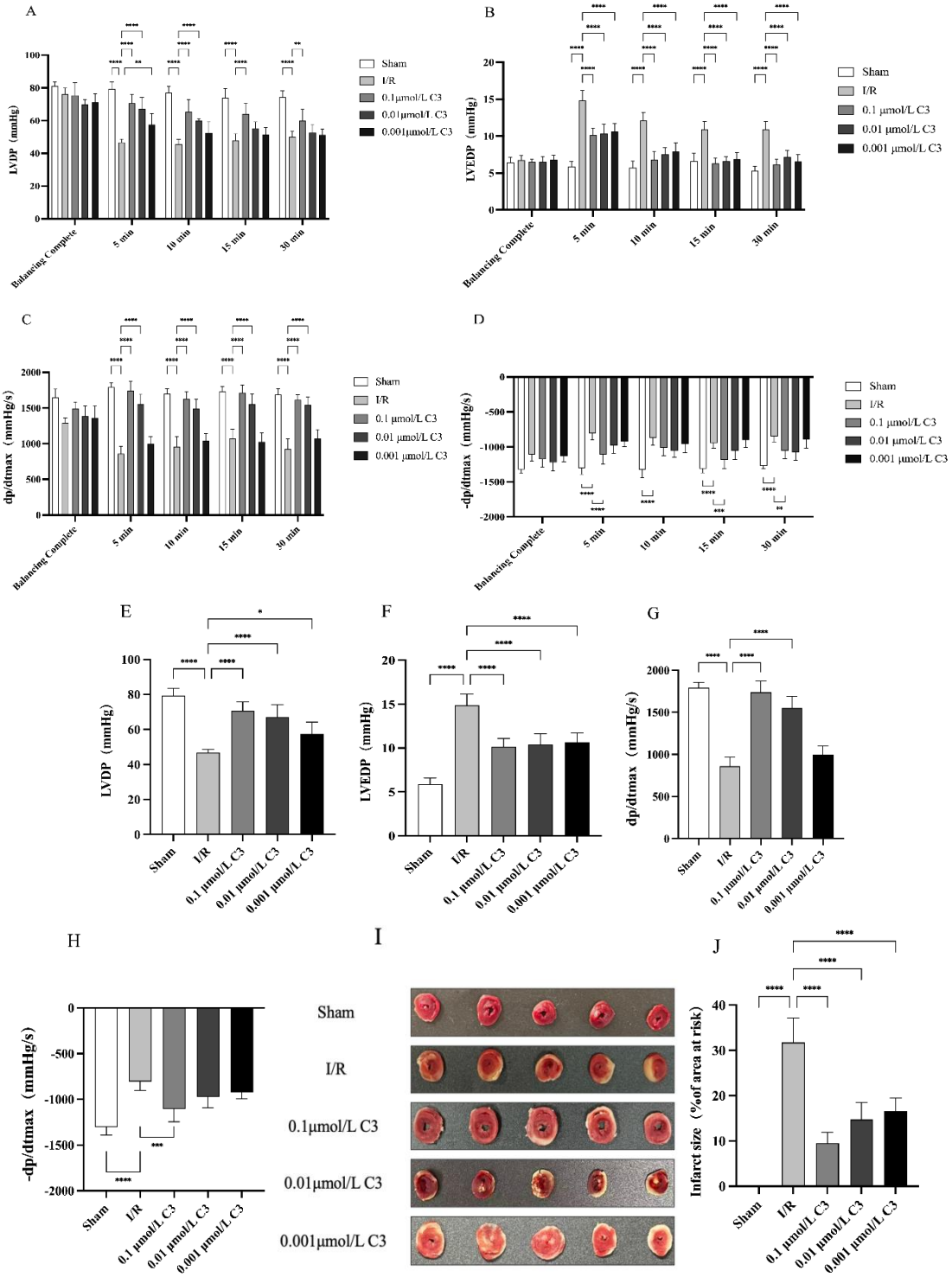


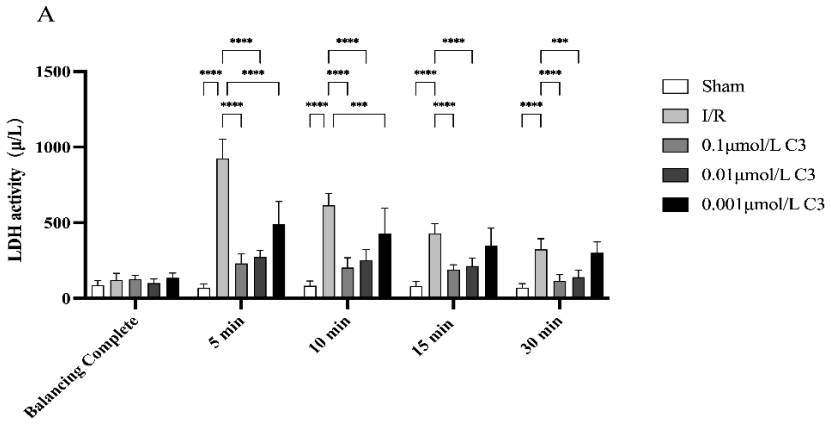
Figure 3. C3 improves cardiac contractile function and decreases myocardial infarct size in ex vivo MIRI models. (A–D) Dynamic alterations of hemodynamic indicators at five reperfusion time in the Sham, I/R, and C3 treatment groups with serial concentrations (n = 6 per group). LVDP, left ventricular diastolic pressure; LVEDP, left ventricular end-diastolic pressure; +dp/dtmax, maximum rate of left ventricular pressure rise; -dp/dtmax, maximum rate of left

ventricular pressure decline. (E–H) Hemodynamic indicators measured at 5 min post-reperfusion in the Sham, I/R, and C3-treated subgroups (n = 6 per group). (I) Representative TTC-stained myocardial slices from all experimental groups (n = 6 per group). (J) Quantitative statistical analysis of myocardial infarct area across groups (n = 6 per group). $^{****}P < 0.0001$, $^{***}P < 0.005$, $^{**}P < 0.01$.

3.2. C3 alleviated tissue injury and oxidative stress induced by ex vivo MIRI

LDH release during MIRI acts as a critical marker of myocardial metabolic disturbance and cardiomyocyte damage. Oxidative stress injury is a typical pathological feature of MIRI, driven by disrupted cardiac antioxidant homeostasis. This imbalance triggers massive reactive oxygen species (ROS) buildup and subsequent myocardial tissue injury. LDH, MDA and SOD were detected to evaluate tissue damage and oxidative stress status.

The results showed that LDH activity in the I/R group was markedly elevated at 5, 10, 15, and 30 min post-reperfusion (Figure 4A); Relative to the I/R group, all C3 dosage groups displayed suppressed LDH leakage in a concentration-dependent manner (Figure 4A).Tissue injury peaked at 5 min post-reperfusion, so this time point was chosen for follow-up biomarker detection (Figure 4B). Cardiac MDA content and SOD activity were further quantified to evaluate oxidative stress. The I/R group exhibited higher MDA levels (Figure 4C) and lower SOD activity (Figure 4D). Treatment with serial concentrations of C3 reversed these alterations: MDA levels declined while SOD activity rose to different extents compared with untreated I/R hearts. Among all doses, 0.1 μmol/L C3 exerted the strongest regulatory effect on both antioxidant indicators (Figure 4C, D).



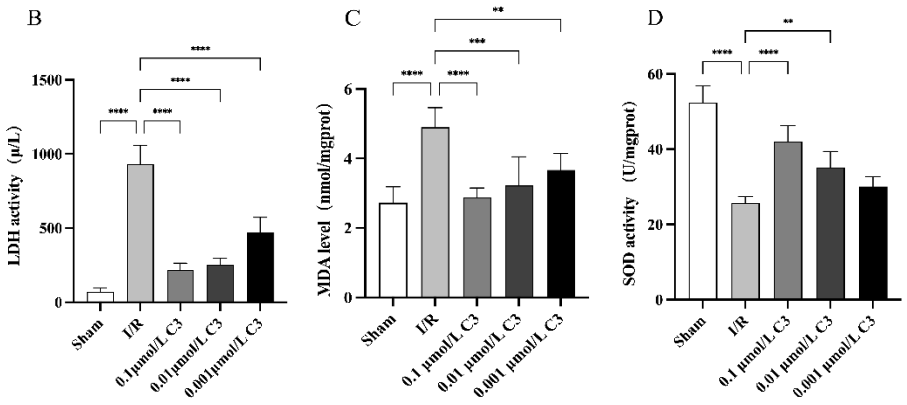


Figure 4. Effects of C3 on LDH release, MDA content and SOD activity in ex vivo rat hearts with MIRI injury. (A) LDH activity measured at five reperfusion time points in Sham, I/R and serially diluted C3 treatment groups (n = 6 per group). (B) LDH activity at 5 min after reperfusion across all groups (n = 6 per group). (C) Myocardial MDA levels of each group (n = 6 per group). (D) Myocardial SOD activity of each group (n = 6 per group). $^{****}P < 0.0001$, $^{***}P < 0.005$, $^{**}P < 0.01$.

3.3. C3 alleviated in vivo MIRI injury, suppressed oxidative stress, and reduced myocardial infarct size

The ex vivo Langendorff MIRI model confirmed the cardioprotective properties of C3, yet this isolated heart system could only reflect direct drug effects on the myocardium. Considering that systemic organs and neurohumoral regulation collectively mediate drug efficacy under physiological conditions, an in vivo rat MIRI model was constructed to comprehensively validate C3's protective function. Successful model establishment was confirmed by characteristic ST-segment elevation on electrocardiography (ECG) (Figure 5A).

TTC staining was conducted to quantify myocardial infarct area. Larger infarct regions were observed in the I/R group (Figure 5B, C), whereas C3 administration at serial doses markedly diminished infarct size in all treatment subgroups (Figure 5B, C). Serum biochemical detection revealed drastically increased LDH and MDA concentrations, alongside suppressed SOD activity in untreated I/R rats (Figure 5D – F). Relative to the I/R group, C3 intervention lowered serum LDH and MDA levels and restored SOD activity in a dose-dependent manner (Figure 5D – F). Among all tested doses, 0.5 mg/kg C3 exerted the optimal regulatory effect on all three injury and oxidative stress biomarkers.

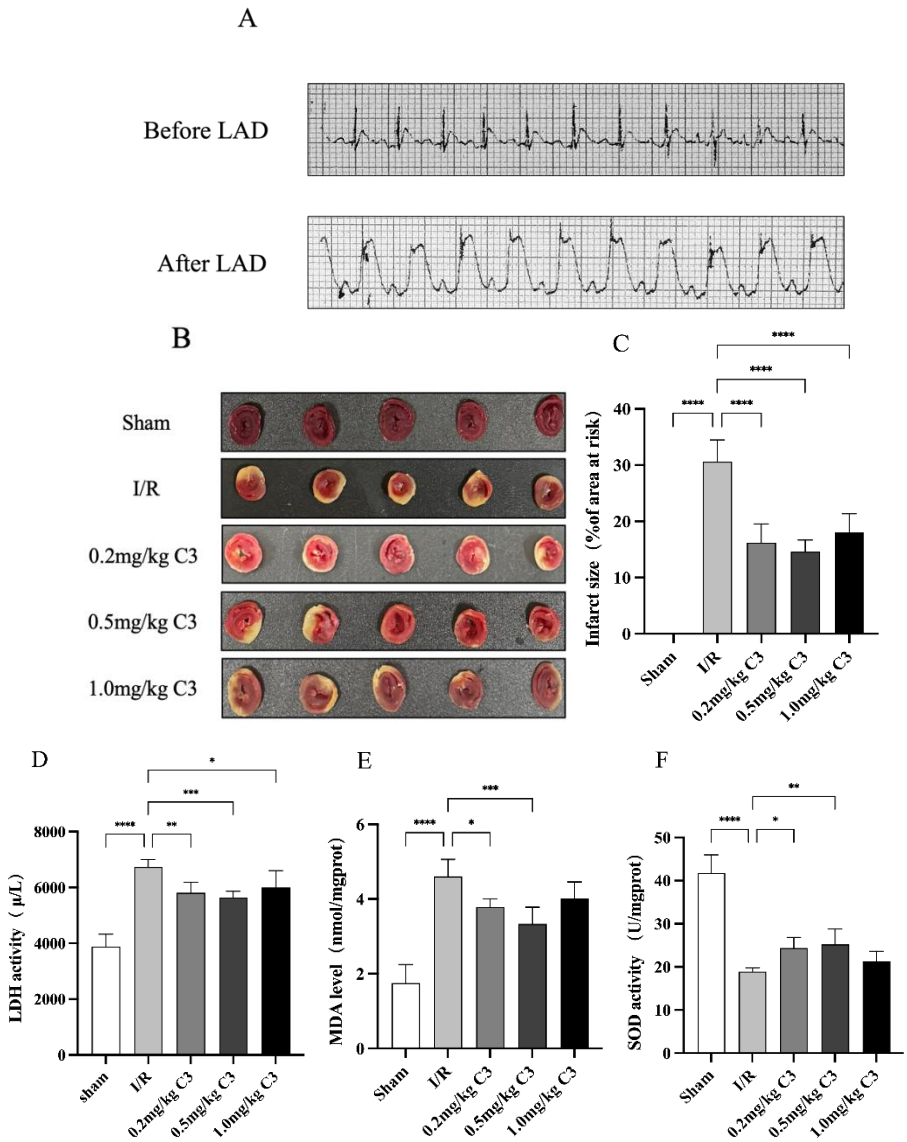


Figure 5. C3 mitigates oxidative stress-induced myocardial injury and limits infarct size in vivo MIRI models. (A) Representative ECG traces before and after left anterior descending artery (LAD) ligation. (B) Representative TTC-stained myocardial slices of all experimental groups (n = 6 per group). (C) Quantitative statistical analysis of myocardial infarct area of each group (n = 6 per group). (D) Serum LDH activity of each group (n = 6 per group). (E) Myocardial MDA content of each group (n = 6 per group). (F) Myocardial SOD activity of each group (n = 6 per group). $^{****}P < 0.0001$, $^{***}P < 0.005$, $^{**}P < 0.01$, $^{*}P < 0.05$.

3.4. Intervention in the TRPM7 pathway regulated C3-mediated cardio protection against ex vivo MIRI.

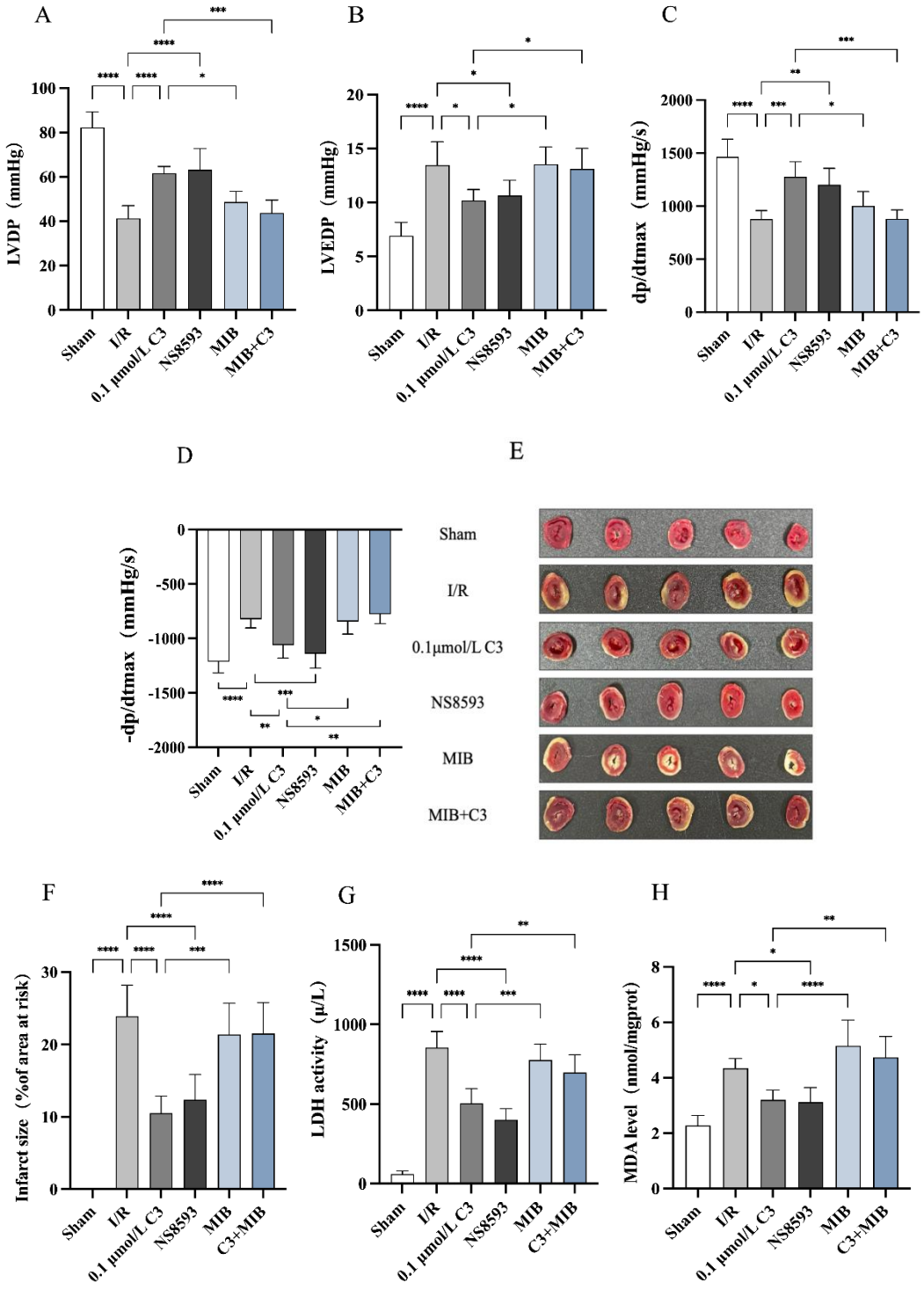
After identifying the optimal C3 concentration in the ex vivo MIRI model, we set up three additional experimental groups: a TRPM7 inhibitor (NS8593) group, a TRPM7 agonist (Mibefradil, MIB) group, and an MIB + C3 co-treatment group. This series of interventions was designed to verify whether TRPM7 serves as the core target through

which C3 exerts cardioprotective activity. We evaluated cardiac function, myocardial injury and oxidative stress to confirm this regulatory axis. After identifying the optimal C3 concentration in the ex vivo MIRI model, we set up three additional experimental groups: a TRPM7 inhibitor (NS8593) group, a TRPM7 agonist (Mibefradil, MIB) group, and MIB + C3 co-treatment group. This series of interventions was designed to verify whether TRPM7 serves as the core target through which C3 exerts cardioprotective activity. We evaluated cardiac function, myocardial injury and oxidative stress to confirm this regulatory axis.

Hemodynamic detection revealed that relative to the Sham group, the I/R group exhibited marked declines in LVDP, +dp/dtmax and −dp/dtmax, alongside a prominent rise in LVEDP. Treatment with 0.1 μmol/L C3 remarkably restored all impaired cardiac functional indices; the NS8593 group yielded similar protective phenotypes. In contrast, MIB monotherapy and MIB + C3 co-treatment abolished the beneficial effects of C3, accompanied by suppressed LVDP, +dp/dtmax and −dp/dtmax as well as a striking secondary elevation in LVEDP (Figure 6A – D).

Myocardial infarct size and LDH leakage assays demonstrated enlarged infarct regions and elevated LDH activity in I/R hearts. Supplementation with 0.1 μ mol/L C3 or NS8593 alleviated these injuries, whereas such protective improvements were eliminated in both the MIB and MIB + C3 groups (Figure 6E – G).

Biochemical assessment of oxidative stress showed increased MDA levels and diminished SOD activity in the I/R myocardium. Compared with the I/R group, C3 and NS8593 treatment lowered MDA accumulation and recovered SOD activity. However, these antioxidant benefits were abrogated in MIB and MIB + C3 co-treatment groups, which displayed higher MDA and lower SOD levels (Figure 6H, I).


A
LVDP（mmHg）
B
LVEDP（mmHg）
C
dp/dtmax（mmHg/s）
Sham
I/R
0.1 μmol/L C3
NS8593
MIB
MIB+C3
D
-dp/dtmax（mmHg/s）
E
Sham
I/R
0.1μmol/L C3
NS8593
MIB
MIB+C3
F
Infarct size（%of area at risk）
C3+MIB
G
LDH activity（μ/L）
H
MDA level（nmol/mgprot）

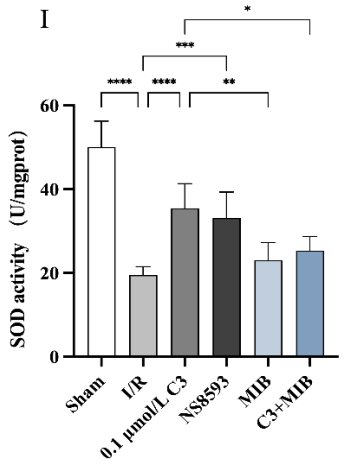


Figure 6. C3 exerts cardio protection against ex vivo MIRI via regulation of the TRPM7 channel. (A) Changes in LVDP at 5 min of reperfusion in each group (n = 6 per group). (B) Changes in LVEDP at 5 min of reperfusion in each group (n = 6 per group). (C) Changes in +dp/dtmax at 5 min of reperfusion in each group (n = 6 per group). (D) Changes in -dp/dtmax at 5 min of reperfusion in each group (n = 6 per group). LVDP, left ventricular diastolic pressure; LVEDP, left ventricular end-diastolic pressure; +dp/dtmax, maximum rate of rise of left ventricular pressure; -dp/dtmax, maximum rate of fall of left ventricular pressure. (E) Representative TTC- stained myocardial sections from each group (n = 6 per group). (F) Quantitative statistical analysis of myocardial infarction area of each group (n = 6 per group). (G) Myocardial LDH activity in each group (n = 6 per group). (H) Myocardial MDA content of each group (n = 6 per group). (I) Myocardial SOD activity of each group (n = 6 per group). $^{****}P < 0.0001$, $^{***}P < 0.005$, $^{**}P < 0.01$, $^{*}P < 0.05$.

3.5. C3 regulated the TRPM7 protein abundance in myocardial tissue of ex vivo MIRI rats

Western blot assays were conducted to clarify whether TRPM7 serves as the direct molecular target underlying C3-mediated cardio protection. TRPM7 protein abundance was significantly increased in myocardial tissues of the I/R group, while 0.1 μ mol/L C3 treatment markedly suppressed TRPM7 expression. The NS8593 group exhibited a similar inhibitory trend against TRPM7 upregulation, and both the C3 and NS8593 groups displayed notably lower TRPM7 levels relative to the I/R group; in contrast, TRPM7 protein was significantly restored in both the MIB monotherapy and MIB + C3 co-treatment groups when compared with the C3-only group (Figure 7A, B). This finding confirmed that C3 suppressed MIRI-triggered TRPM7 overexpression, and TRPM7 represented a core target responsible for C3's cardioprotective activity.

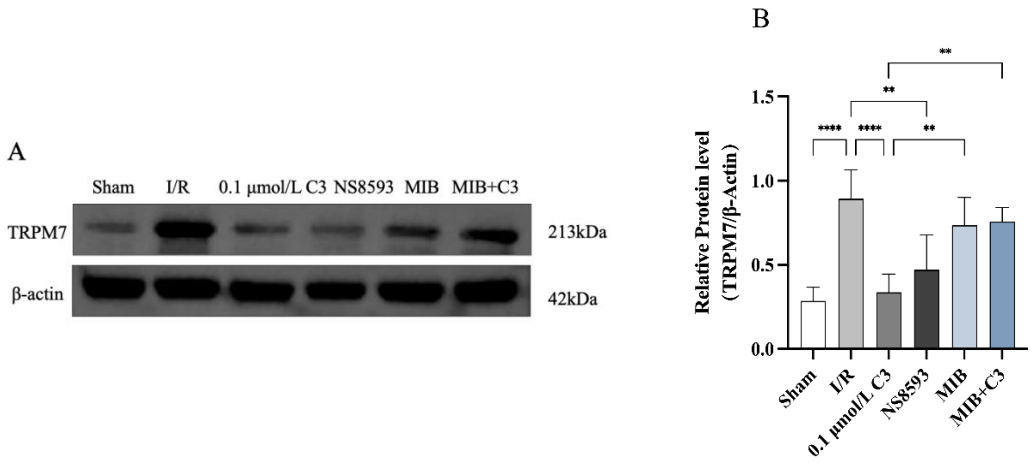


Figure 7. Graphs showing TRPM7 protein expression levels and quantification. (A) Western blot analysis of TRPM7 (n = 5 per group). (B) TRPM7 expression levels (n = 5 per group). $^{****}P < 0.0001$, $^{**}P < 0.01$.

3.6. C3 alleviated ex vivo MIRI and suppressed cardiomyocyte apoptosis via TRPMP inhibition and Nrf2 pathway activation

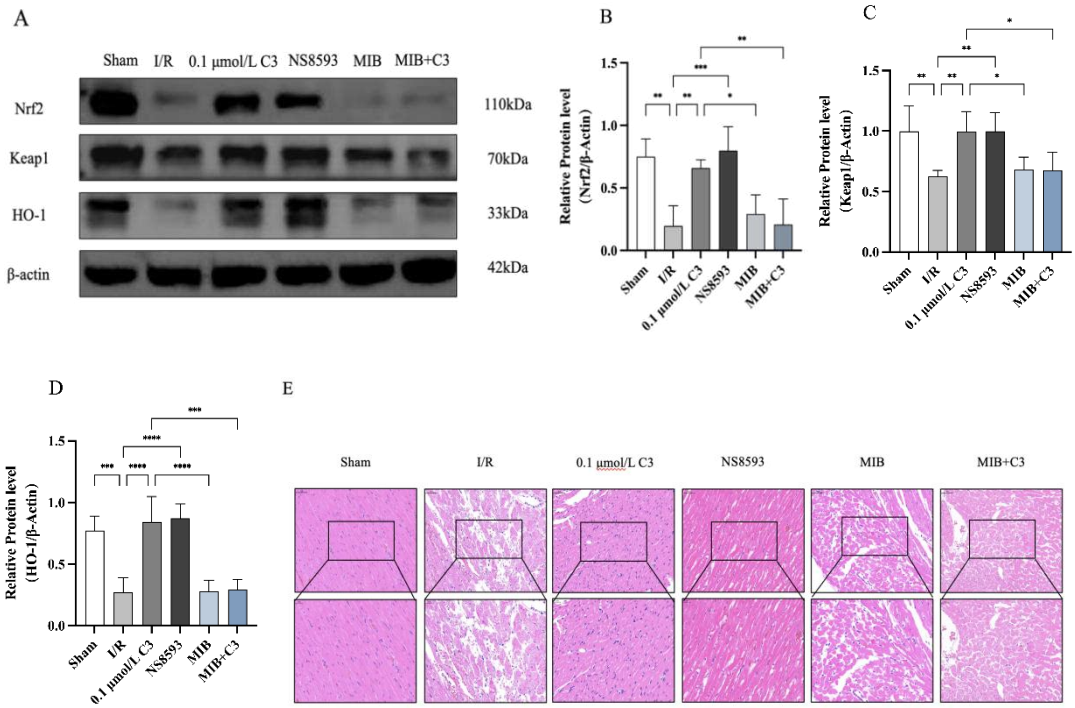
As a key transcription factor governing oxidative stress response, Nrf2 orchestrates the central antioxidant defense network by regulating the transcription of downstream antioxidant genes. Western blot detection revealed altered abundance of Nrf2, Keap1 and HO-1 in myocardial tissues. Western blot results revealed altered abundance of Nrf2, Keap1 and HO-1 in myocardial tissues. Compared with the Sham group, the I/R group displayed markedly downregulated Nrf2 and HO-1 alongside elevated Keap1 levels. Treatment with 0.1 μmol/L C3 robustly upregulated all three proteins, implying activation of the Nrf2 antioxidant axis; consistently, the TRPM7 inhibitor NS8593 produced identical regulatory trends. In contrast, co-administration of the TRPM7 agonist Mibefradil (MIB) abolished C3-triggered Nrf2 signaling activation. These observations confirmed that C3 exerted cardio protection against ex vivo MIRI by suppressing TRPM7 to initiate Nrf2-mediated antioxidant responses. (Figure 8A–D).

Apoptosis is one of the hallmarks of MIRI. To clarify whether C3 confers anti-apoptic benefits through TRPM7 suppression, hematoxylin-eosin (HE) staining was performed to examine cardiomyocyte morphological alterations. Cardiomyocytes from Sham hearts exhibited regular alignment and intact cellular architecture. In contrast, I/R injury induced disorganized myofibers, widened intercellular spaces and visible

myocardial fiber rupture. Both 0.1 μmol/L C3 and NS8593 partially rescued these morphological abnormalities and restored cardiomyocyte arrangement. However, MIB and MIB+C3 co-treatment aggravated tissue injury, featured by widened intercellular spaces, and cytoplasmic vacuolization (Fig. 8E).

TUNEL staining was further applied to quantify apoptotic cardiomyocytes. The I/R group presented a drastically elevated apoptotic index compared with the Sham group. C3 and NS8593 intervention both reduced the proportion of apoptotic cells, whereas co-treatment with MIB abrogated C3's anti-apoptotic phenotype (Figure 8F, G). Western blot quantification of apoptosis-related proteins further validated these TUNEL results. Compared with Sham samples, I/R myocardium showed reduced anti-apoptotic Bcl-2 abundance and increased pro-apoptotic Bax and cleaved caspase-3 levels. C3 or NS8593 treatment reversed these changes: Bcl-2 was upregulated, while Bax and cleaved caspase-3 were downregulated relative to the I/R group. Compared with the C3-only group, the MIB + C3 combination group displayed suppressed Bcl-2 expression and accumulated Bax and cleaved caspase-3 (Figure 8H – K).

Collectively, these data demonstrated that C3 mitigated ex vivo myocardial I/R injury by inhibiting TRPM7 and activating the Nrf2 antioxidant cascade, thereby attenuating cardiomyocyte apoptosis.



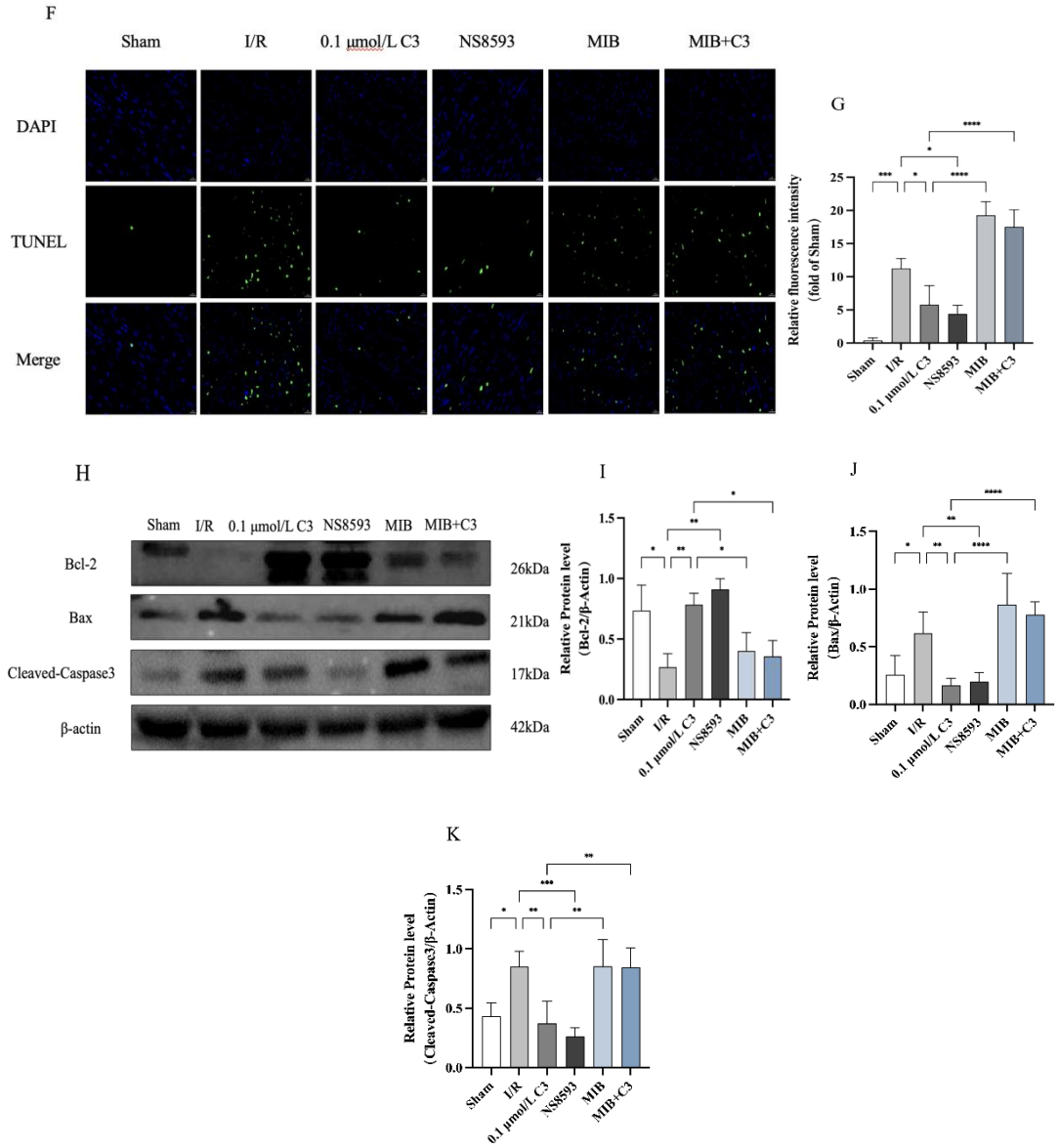


Figure 8. C3 upregulates Nrf2 pathway protein abundance and suppresses MIRI-triggered cardiomyocyte apoptosis in ex vivo cardiac tissues. (A) western blot of Nrf2, Keap1 and HO-1 from ex vivo cardiac tissues of all groups. Representative Western blot bands of Nrf2, Keap1, and HO-1 from ex vivo cardiac tissues of all groups. (B–D) Quantitative statistical analysis of Nrf2, Keap1, and HO-1 protein levels (Nrf2 n = 4, Keap1 n = 5, HO-1 n = 4). (E) Hematoxylin and eosin (HE) staining of cardiac tissue sections(scale bar 50 μm). (F) Representative TUNEL immunofluorescence images of myocardial tissues (green: TUNEL-positive apoptotic cells; blue: DAPI nuclear staining; scale bar 20 μm). (G) Quantification of TUNEL-positive apoptotic cell ratio (n = 3 per group) Quantification of TUNEL -positive apoptotic cell ratio (n = 3 per group). (H) Representative western blot bands of Bcl-2, Bax, and Cleaved-Caspase3 across groups (I–K) Quantitative analysis of Bcl-2, Bax, and Cleaved-Caspase3 expression (Bcl-2 n = 3, Bax n = 5, Cleaved-Caspase3 n = 4). $^{****}P < 0.0001$, $^{***}P < 0.005$, $^{**}P < 0.01$, $^{*}P < 0.05$.

3.7. TRPM7 pathway intervention modulated C3-conferred cardio protection against in vivo MIRI injury

To validate whether TRPM7 acts as the functional target mediating C3’s cardio

protection in the in vivo MIRI model, three additional cohorts were established: a TRPM7 inhibitor (NS859) group, a TRPM7 agonist (MIB) group, and an MIB + C3 co-treatment group. TTC staining and serum LDH activity assays demonstrated enlarged infarct area and elevated LDH leakage in untreated I/R rats. Supplementation with 0.5 mg/kg C3 or NS8593 alleviated both injuries, whereas co-administration of MIB abolished the beneficial outcomes induced by C3 (Fig. 9A–C).

Biochemical detection of oxidative stress biomarkers revealed drastically higher MDA levels and suppressed SOD activity in the I/R group relative to the Sham group. C3 or NS8593 intervention markedly lowered MDA accumulation and recovered SOD activity; however, MIB co-treatment counteracted these antioxidant effects of C3, resulting in a secondary rise in MDA levels and further reduction of SOD activity (Figure 9 D, E).

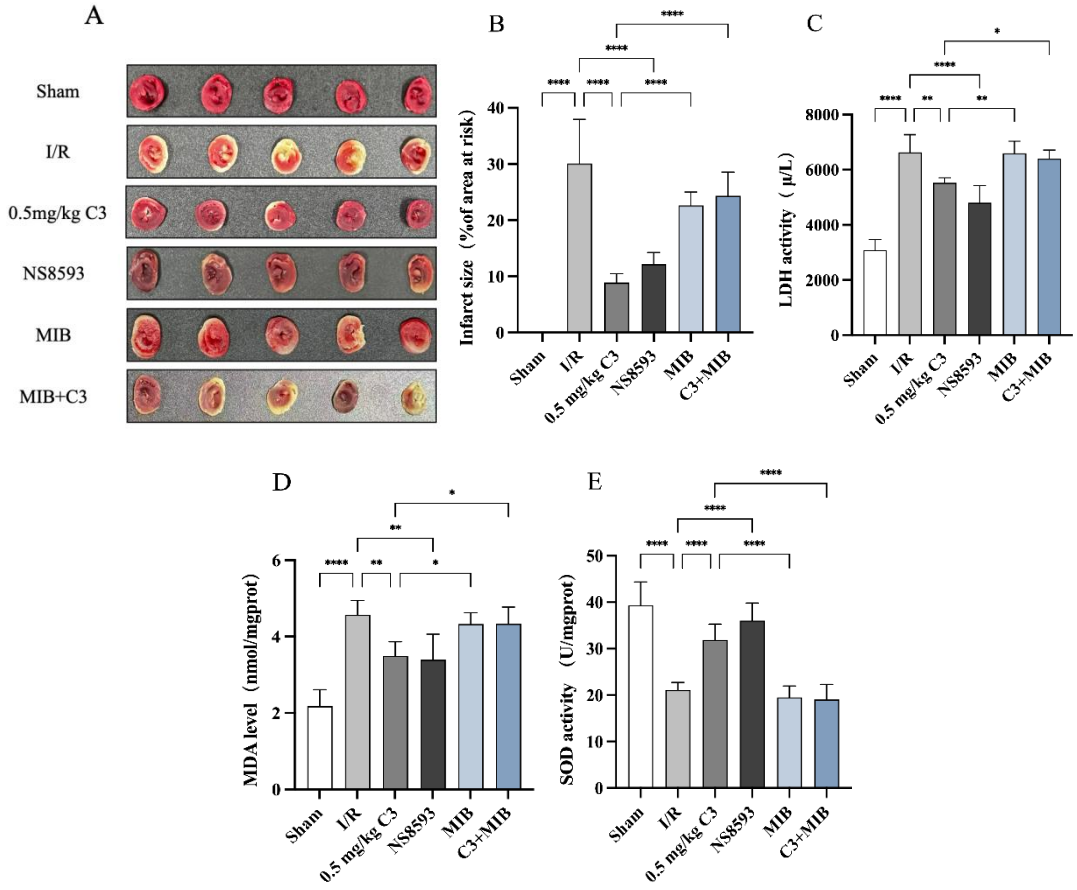


Figure 9. C3 exerts cardio protection against in vivo MIRI via modulation of the TRPM7 channel. (A) Representative TTC-stained myocardial slices of all experimental groups (n = 6 per group). (B) Quantitative statistical analysis of myocardial infarction area across groups (n = 6 per group). (C) Myocardial LDH activity in each group (n = 6 per group). (D) Myocardial MDA content in each group (n = 6 per group). (E) SOD activity in

each group (n = 6 per group). $^{****}P < 0.0001$, $^{***}P < 0.005$, $^{**}P < 0.01$, $^{*}P < 0.05$.

3.9. C3 modulated TRPM7 protein abundance in myocardial tissue of in vivo MIRI rats

Western blot assays were performed to identify whether TRPM7 serves as the direct molecular target underlying C3-mediated cardio protection. TRPM7 protein abundance was significantly higher in myocardial tissues of the I/R group relative to the Sham group; following 0.5 mg/kg C3 intervention, TRPM7 levels were remarkably suppressed. Treatment with the TRPM7 inhibitor NS8593 yielded a comparable inhibitory effect on TRPM7 overexpression versus untreated I/R hearts. In contrast, TRPM7 agonist MIB abrogated C3-induced TRPM7 downregulation. Both the MIB monotherapy and MIB + C3 co-treatment groups exhibited significantly restored TRPM7 expression relative to the C3-only group (Figure 10A, B). These findings confirmed that TRPM7 acts as a core target responsible for C3's cardioprotective activity, and C3 efficiently suppressed in vivo MIRI-triggered TRPM7 upregulation.

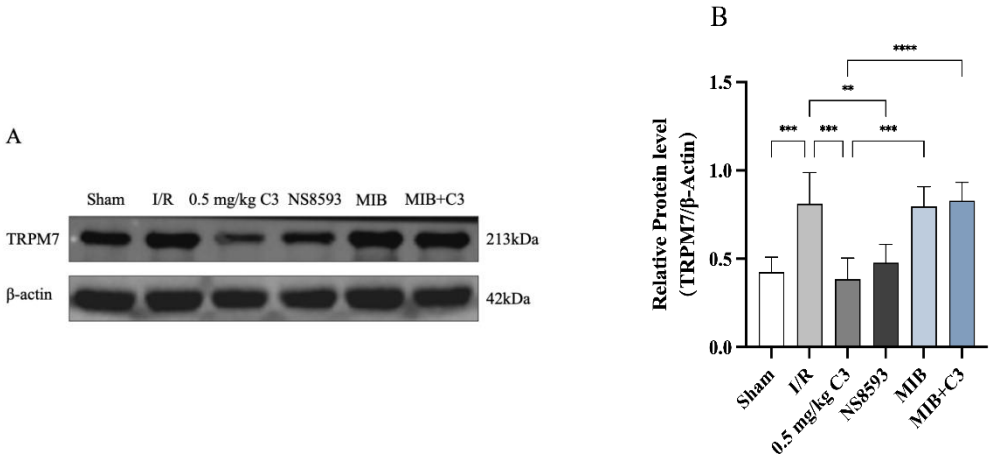


Figure 10. Graphs showing TRPM7 protein expression levels and quantification. (A) Western blot analysis of TRPM7 (n = 5 per group). (B) TRPM7 expression levels (n = 5 per group). $^{****}P < 0.0001$, $^{***}P < 0.005$, $^{**}P < 0.01$.

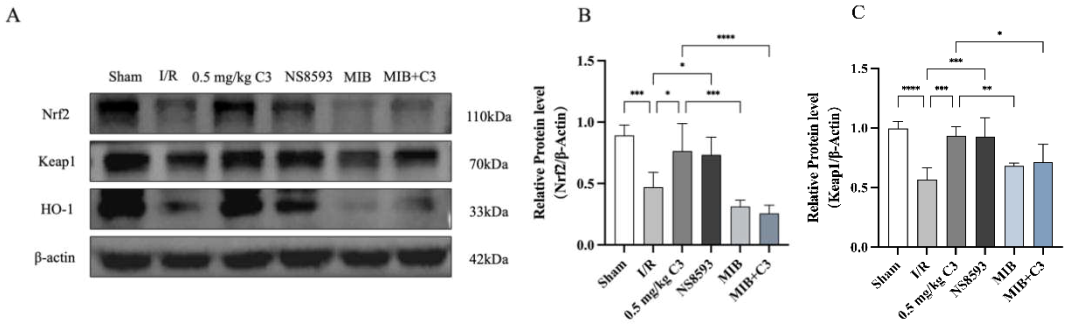
3.10. C3 alleviated in vivo MIRI and suppressed cardiomyocyte apoptosis via TRPM7 inhibition and Nrf2 signaling pathway activation

Consistent with our ex vivo MIRI findings, western blot assays were performed to detect core proteins of the Nrf2 antioxidant cascade. Nrf2 signaling was markedly

suppressed in myocardial tissues from I/R rats. Treatment with 0.5 mg/kg C3 or the TRPM7 inhibitor NS8593 robustly restored pathway activity. However, co-administration of the TRPM7 agonist MIB abolished C3-mediated Nrf2 activation, accompanied by reduced protein abundance of Nrf2 and HO-1 alongside elevated Keap1 levels (Figure 11A–D).

HE staining showed regular alignment and intact morphology of cardiomyocytes in the Sham group. By contrast, I/R injury induced disorganized myofibers, enlarged intercellular gaps and overt myocardial fiber laceration. C3 or NS8593 intervention mitigated these pathological injuries and restored relatively ordered cardiomyocyte structure. Conversely, MIB monotherapy and MIB + C3 co-treatment aggravated tissue damage, with recurrent widened interstitial spaces and broken cardiac fibers observed (Figure 11E).

TUNEL staining revealed a markedly higher apoptotic index in the I/R group relative to the Sham group. Both C3 and NS8593 markedly lowered the proportion of apoptotic cardiomyocytes, while the MIB and MIB + C3 groups displayed elevated apoptotic levels compared with the C3-only cohort (Figure 11F, G). Follow-up western blot quantification of apoptosis-related proteins further validated these phenotypes: C3 and NS8593 suppressed cardiomyocyte apoptosis, whereas MIB counteracted such protective effects, as reflected by upregulated pro-apoptotic protein expression (Figure 11H – K).



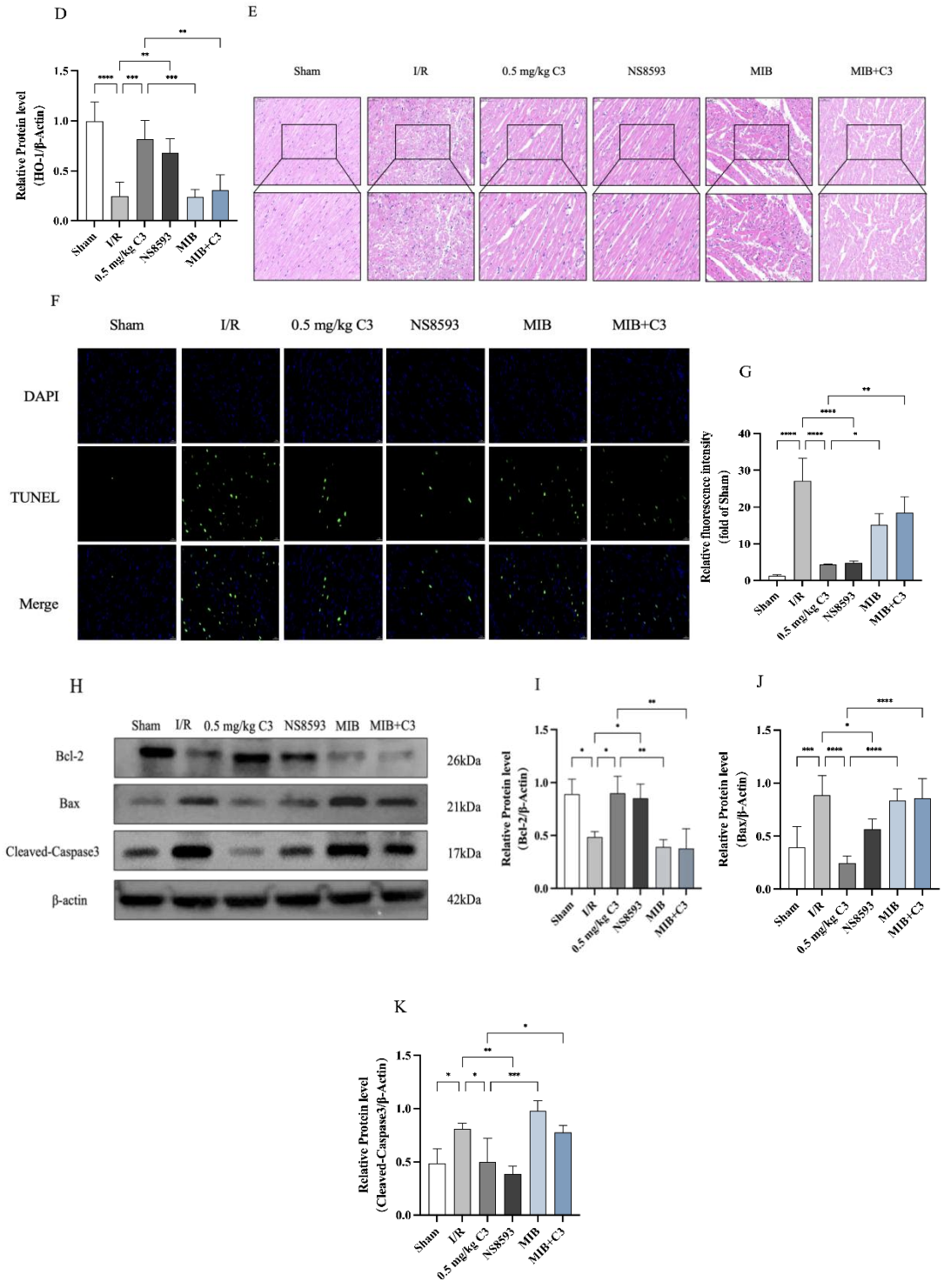


Figure 11. C3 upregulates Nrf2 pathway protein abundance and alleviates cardiomyocyte apoptosis after in vivo MIRI injury. (A) Representative western blot bands of Nrf2, Keap1, and HO-1 in myocardial tissue of all groups. (B–D) Quantitative statistical analysis of Nrf2, Keap1 and HO-1 protein levels (Nrf2 n = 5, Keap1 n = 5, HO-1 n = 4). (E) Representative hematoxylin and eosin (HE) staining in myocardial tissue of all groups (scale bar = 50 μm). (F) Representative TUNEL immunofluorescence images of myocardium (green: TUNEL-positive apoptotic cells; blue: DAPI nuclear staining; scale bar = 20 μm). (G) Quantitative statistical analysis of TUNEL-positive apoptotic cell ratio (n = 3 per group). (H) Representative western blot bands of Bcl-2, Bax, and Cleaved-Caspase3 from myocardial tissues of each group. (I–K) Quantitative statistical analysis of Bcl-2, Bax and Cleaved-Caspase3 across

groups (Bcl-2 n = 3, Bax n = 5, Cleaved-Caspase3 n = 4). $^{****}P < 0.0001$, $^{***}P < 0.005$, $^{**}P < 0.01$, $^{*}P < 0.05$.

Discussion

MIRI represents a common adverse complication of myocardial ischemia reperfusion therapy and severely affects long-term prognostic outcomes in patients. Although timely thrombolysis and interventional procedures effectively restore myocardial blood perfusion, subsequent pathological cascades, including ROS overproduction, Ca^{2+} overload within cells, and inflammatory activation, further aggravate cardiac dysfunction and ultimately trigger extensive cardiomyocyte death[4]. Accumulating studies have focused on the molecular and cellular mechanisms underlying MIRI pathogenesis, among which oxidative stress is well recognized as a key driver of myocardial injury[31]. Over the past few years, naturally occurring bioactive substances have attracted considerable interest as potential cardioprotective candidates for treating MIRI. As the principal bioactive constituents of ginseng, ginsenosides display a broad spectrum of pharmacological actions, such as anti-inflammatory and antioxidative effects[9]. Specifically, ginsenoside aglycones Rg3 and Rh2 have been validated to alleviate myocardial I/R injury[10, 11]. Consistent with these findings, Li et al. [32] found that ginsenoside Rg3 effectively reduces myocardial infarct size, preserves left ventricular function, and alleviates MIRI progression, while, ginsenoside Rh2 attenuates myocardial infarction, improves ventricular contractility, and inhibited myocardial fibrosis[33]. Nevertheless, the clinical translational application of native ginsenoside aglycones is largely restricted by limited natural sources and high purification costs. Advances in isolation and synthesis techniques have recently facilitated the development of semi-synthetic ginsenoside derivatives as novel therapeutic candidates[33]. In this study, we synthesized a novel semi-synthetic ginsenoside derivative, Compound 3 (C3), which integrates the structural characteristics of both Rg3 and Rh2 aglycones[12].

This work was designed to comprehensively assess the protective effects of C3 on MIRI and to elucidate the molecular pathways involved, thereby offering preclinical

support for the development of new anti-MIRI therapies.

To comprehensively evaluate the protective effects of C3, two classic and complementary MIRI models were established in this study: an ex vivo Langendorff-perfused rat heart model and an in vivo rat model constructed via ligation of the left anterior descending coronary artery. Functional assessment demonstrated that C3 pretreatment significantly rescued impaired cardiac contractile and diastolic function in ex vivo MIRI. as evidenced by restored LVDP and ±dp/dtmax, alongside reduced LVEDP. Moreover, C3 markedly reduced myocardial infarct size and decreased LDH leakage in both ex vivo and in vivo MIRI models, indicating its direct protective action against myocardial I/R damage. Given that the ex vivo Langendorff system excludes systemic neurohumoral regulation and only reflects direct drug effects on isolated hearts, the in vivo MIRI model was further adopted to simulate the complex physiological microenvironment of myocardial ischemia and reperfusion. In vivo experimental results confirmed that C3 effectively ameliorated MIRI-associated oxidative stress, as demonstrated by reduced myocardial infarct size, decreased serum MDA levels and LDH activity, and elevated antioxidant SOD activity. Collectively, these findings indicate that the cardioprotective capacity of C3 is closely attributed to its potent antioxidant properties.

TRPM7 is a dual-function protein exhibiting both cation channel and kinase activities, which participates extensively in the pathogenesis of multiple cardiovascular diseases [18]. Growing evidence has verified that TRPM7 is significantly upregulated during I/R injury, and TRPM7-mediated Ca^{2+} influx triggers mitochondrial dysfunction and excessive oxidative stress, ultimately inducing cardiomyocyte death.[34, 35]. Mechanistically, previous mechanistic studies have in validated the pathological role of TRPM7 in MIRI. Deng et al. [36] reported that in hypoxia/reoxygenation (H/R)-induced AC16 cardiomyocytes, dysregulation of the miR-335-5p/TRPM7 axis augments cellular damage, whereas pharmacological inhibition of TRPM7 efficiently reverses H/R-induced injury. In addition, LI et al. [34] demonstrated that TRPM7 upregulation exacerbates myocardial infarction and cardiomyocyte apoptosis in an ex vivo I/R model, and TRPM7 inhibition by 2-APB substantially improves cardiac functional recovery.

Consistently, multiple studies have confirmed that TRPM7 exacerbates H/R-induced myocardial damage by facilitating Ca^{2+} influx and activating downstream calcium-dependent signaling cascades[35]. In mouse MIRI models, TRPM7 overexpression is, accompanied by cardiac dysfunction, myocardial structural damage, and increased apoptotic rates, while TRPM7 inhibition via Waixenicin A efficiently alleviates MIRI pathological phenotypes. These studies collectively establish TRPM7 as a pathogenic mediator of MIRI. In line with previous reports, our Western blot results revealed significant TRPM7 protein upregulation in I/R-injured myocardial tissues, whereas C3 intervention significantly suppressed TRPM7 abundance, suggesting that TRPM7 may serve as a core target for C3-mediated cardio protection.

To gain further evidence for the causal link between modulation of TRPM7 and the protective actions of C3, pharmacological rescue experiments were performed using the specific TRPM7 inhibitor NS8593 and agonist MIB. Our results showed that NS8593 treatment recapitulated the cardioprotective phenotypes of C3, including restored cardiac performance, diminished infarct area, and attenuated oxidative stress together with reduced cardiomyocyte apoptosis; In contrast, MIB-mediated TRPM7 activation abrogated C3-induced TRPM7 downregulation and partially counteracted the protective effects of C3 against MIRI. These rescue results demonstrate that C3 alleviates MIRI primarily by suppressing TRPM7 expression and activity. Notably, Chubanov et al. [37] demonstrated that NS8593 specifically blocks TRPM7 channel function by interfering with magnesium-dependent gating, which further supports the specific targeting efficiency of NS8593 observed in our study.

During MIRI, apoptosis of cardiomyocytes represents a major mode of cell death, and its regulation is largely dependent on Bcl-2 family members and the caspase signaling cascade. Mitochondrial vulnerability to apoptosis is governed by the ratio of pro-apoptotic Bax to anti-apoptotic Bcl-2, while caspase-3 act as the final effector that executes apoptotic progression, whose expression level directly reflects the severity of myocardial apoptosis[38]. In this study, HE staining and Western blot assays were applied to assess the regulatory effects of C3 on cardiomyocyte apoptosis and its correlation with TRPM7 activity. Morphological observations showed that C3

pretreatment alleviated I/R-induced myocardial structural disorder, restored orderly cardiomyocyte arrangement, and narrowed widened intercellular gaps. At the molecular level, C3 significantly upregulated the expression of Bcl-2 and downregulated the levels of pro-apoptotic Bax and Cleaved-Caspase3. These findings are consistent with a previous study reporting that Rg3 alleviates I/R-induced cardiomyocyte ferroptosis by modulating the Bax/Bcl-2 balance[21]. Further pharmacological intervention verified that NS8593, a TRPM7 inhibitor, mimicked the anti-apoptotic effects of C3, whereas MIB-induced TRPM7 activation abolished C3-mediated anti-apoptotic activity. Taken together, these results demonstrate that C3 suppresses MIRI-triggered cardiomyocyte apoptosis in a TRPM7-dependent manner. Having confirmed the TRPM7-dependent cardioprotective and anti-apoptotic effects of C3, we further explored the downstream antioxidant signaling mechanism. The Nrf2-Keap1-HO-1 cascade is the core regulatory axis of intracellular antioxidant defense. Under physiological conditions, Nrf2 is constitutively bound to Keap1, undergoing continuous ubiquitination and proteasomal degradation. Upon oxidative stress stimulation, Keap1 conformational changes trigger Nrf2 dissociation and, nuclear transcription, thereby initiating the transcription of downstream antioxidant genes such as HO-1 to restore redox homeostasis[22, 23]. Previous studies have demonstrated that natural ginsenosides Rh2 and Rg3 exert anti-MIRI and antioxidant effects by activating the Nrf2-Keap1 signaling pathway[11, 21]. Based on our phenotypic findings that C3 effectively mitigates MIRI-associated oxidative damage, we further detected the expression profiles of Nrf2 pathway proteins. The results verified that C3 treatment significantly activated the Nrf2-Keap1-HO-1 axis, characterized by the of upregulation of Nrf2 and HO-1 and decreased Keap1 abundance. To clarify whether C3 exerts its antioxidant effects via TRPM7, we conducted pharmacological rescue validation. The results showed that TRPM7 inhibition by NS8593 activated Nrf2 antioxidant signaling and phenocopied the antioxidant effects of C3, while TRPM7 activation by MIB blocked C3-mediated Nrf2 pathway activation. Collectively, these data elucidate a novel molecular mechanism: C3 exerts antioxidant cardio protection against MIRI by inhibiting TRPM7 and activating the Nrf2-Keap1-HO-1 signaling cascade.

In this study, dual ex vivo and in vivo MIRI models were adopted to systematically validate the protective efficacy and its underlying molecular mechanisms of C3, ensuring the robustness and reliability of our conclusions. The ex vivo in vitro model eliminated interference of systemic neurohumoral regulation, enabling direct and accurate evaluation of the intrinsic effects of C3 on isolated myocardial tissues. In contrast, the in vivo LAD ligation model recapitulates the complex in vivo pathological microenvironment, incorporating systemic organ crosstalk and neurohumoral regulatory networks. The consistent protective phenotypes observed in two distinct models mutually corroborate the stability and authenticity of C3’s anti-MIRI effects. Furthermore, dual pharmacological verification using TRPM7 inhibitor and agonist clarified the indispensable role of TRPM7 in mediating C3’s cardio protection. Combined with the detection of oxidative stress and apoptosis-related biomarkers, this study systematically elucidates the upstream target and downstream antioxidant signaling pathway of C3.

Despite these meaningful findings, the present study has several limitations that warrant further improvement and in-depth exploration in future research. First, only male SD rats were included in this study. Given the well -documented sex differences in cardiovascular disease susceptibility and drug responsiveness, further validation In female animal models is required to clarify the influence of gender on C3’s protective effects. Second, this study only established an acute MIRI model with 30 min of ischemia followed by 120 min of reperfusion; longer reperfusion durations and multiple time-point interventions should be included in future studies to explore the time-dependent protective profile of C3. Third, the downstream regulatory network of TRPM7 requires further in-depth investigation. As a bifunctional protein with both ion channel and kinase activities, whether the kinase function of TRPM7 participates in modulating C3-mediated Nrf2 activation remains unclear. In addition, whether TRPM7 directly regulates Nrf2 nuclear translocation or synergizes with other classic cardioprotective pathways (e.g., PI3K/Akt and MAPK) needs further validation. Future studies could combine TRPM7-specific kinase inhibition and phosphoproteomics analysis will help systematically elucidate the downstream signaling network of

TRPM7. Fourth, the mechanistic validation of this study is limited to animal tissue levels. No in vitro cardiomyocyte hypoxia/reoxygenation (H/R) model (e.g., primary cardiac myocytes or H9c2 cell lines) was applied to verify the cellular molecular mechanism of C3. Gene overexpression and silencing strategies at the cellular level are needed to further consolidate the causal mechanism. Fifth, this study only adopted pharmacological intervention tools; genetic validation via TRPM7 knockout or knockdown animal models is lacking. Genetic functional verification can provide more rigorous causal evidence for the TRPM7-dependent mechanism of C3. Finally, recent studies have reported that ginsenosides regulate multiple cell death modes, including ferroptosis[21, 39] and pyroptosis[40, 41] to alleviate MIRI. However, the present study only focused on cardiomyocyte apoptosis and oxidative stress; whether C3 modulates ferroptosis, pyroptosis, or other cell death pathways via TRPM7 requires comprehensive exploration in future work.

In summary, this study innovatively clarifies the molecular mechanism of the novel semi-synthetic ginsenoside derivative C3 against MIRI. Mechanistically, C3 suppresses TRPM7 expression and activity, thereby activating the downstream Nrf2-Keap1-HO-1 antioxidant signaling pathway, reducing excessive oxidative stress and cardiomyocyte apoptosis, and ultimately alleviating myocardial I/R injury. These findings provide solid preclinical evidence supporting C3 as a promising candidate for MIRI treatment and identify TRPM7 as a viable therapeutic target for cardiovascular ischemic diseases.

Conclusion

In summary, C3 protects the myocardium against MIRI via TRPM7 inhibition, whereby the TRPM7-regulated Nrf2-Keap1-HO-1 antioxidant signaling pathway suppresses oxidative stress and mediates C3’s cardioprotective effects.

Acknowledgements

Not applicable

Availability of data and materials

The raw/processed data generated in this study are available from the corresponding author upon reasonable request

Authors' contributions

Ziyuan Wang: Writing-original draft, Validation, Methodology, Formal analysis, Conceptualization; Zhiwen Zhou: Resources (provision of ginsenoside derivatives and their synthetic procedures); Ruiyi Luo: Validation; Yongkang Peng: Validation; Caili Zhang: Validation; Qiong Du: Conceptualization, Experimental design, Supervision, Formal analysis, Writing-review & editing; Shizhong Zhang: Conceptualization, Supervision, Writing-review & editing, Funding acquisition.

Ethics approval and consent to participate

Animal care and experimental procedures were performed in accordance with the guidelines of the Animal Ethics Committee of the China Three Gorges University (The animal care license number is SYXK (E) 2017-0061); Clinical trial number: not applicable.

Patient consent for publication

Not applicable

Funding statement

This research was supported by the National Natural Science Foundation of China (No. 30872716), the Natural Science Foundation of Hubei Province, China (No. 2015CFB288), and the Open Foundation of the Hubei Provincial Key Laboratory of Tumor Microenvironment and Immunotherapy (No. 2023KZL06; No. 2024KZL03).

Conflict of Interest

The authors declare that they have no conflicts of interest.

Reference

[1] TSAO C W, ADAY A W, ALMARZOOQ Z I, et al. Heart Disease and Stroke Statistics-2022 Update: A Report From the American Heart Association [J]. Circulation, 2022, 145(8): e153-e639.

[2] XIANG Q, YI X, ZHU X H, et al. Regulated cell death in myocardial ischemia-reperfusion injury [J]. Trends Endocrinol Metab, 2024, 35(3): 219-34.

[3] RAO S V, O'DONOGHUE M L, RUEL M, et al. 2025 ACC/AHA/ACEP/NAEMSP/SCAI Guideline for the Management of Patients With Acute Coronary Syndromes: A Report of the American College of Cardiology/American Heart Association Joint Committee on Clinical Practice Guidelines [J]. Circulation, 2025, 151(13): e771-e862.

[4] OU W, LIANG Y, QIN Y, et al. Hypoxic acclimation improves cardiac redox homeostasis and protects heart against ischemia-reperfusion injury through upregulation of O-GlcNAcylation [J]. Redox Biol, 2021, 43: 101994.

[5] SHI Q, YAO W, ZHANG W, et al. Nrf2 de-SUMOylation alleviates myocardial ischemia-reperfusion injury (MIRI) by attenuating myocardial ferroptosis in mice [J]. Redox Rep, 2026, 31(1): 2624946.

[6] SHI A, ZENG Y, XIN D, et al. Real-Time Visualization of the Antioxidative Potency of Drugs for the Prevention of Myocardium Ischemia-Reperfusion Injury by a NIR Fluorescent Nanoprobe [J]. ACS Sens, 2022, 7(12): 3867-75.

[7] SHARMA A, LEE H J. Ginsenoside Compound K: Insights into Recent Studies on Pharmacokinetics and Health-Promoting Activities [J]. Biomolecules, 2020, 10(7).

[8] CORTÉS H, LIMA E, DUARTE-PEÑA L, et al. Ginsenoside Rg1 as a Multifunctional Therapeutic Agent: Pharmacological Properties, Molecular Mechanisms and Clinical Perspectives in Complementary Medicine [J]. Food Sci Nutr, 2026, 14(2): e71486.

[9] CHEN J, HUANG Q, LI J, et al. Panax ginseng against myocardial ischemia/reperfusion injury: A review of preclinical evidence and potential mechanisms [J]. J Ethnopharmacol, 2023, 300: 115715.

[10] XIA J, CHEN C, DONG M, et al. Ginsenoside Rg3 endows liposomes with prolonged blood circulation and reduced accelerated blood clearance [J]. J Control Release, 2023, 364: 23-36.

[11] FAN Z X, YANG C J, LI Y H, et al. Ginsenoside Rh2 attenuates myocardial ischaemia-reperfusion injury by regulating the Nrf2/HO-1/NLRP3 signalling pathway [J]. Exp Ther Med, 2023, 25(1): 35.

[12] NIU X N, LUO W, LV C N, et al. Research progress on naturally-occurring and semi-synthetic ocotillol-type ginsenosides in the genus Panax L. (Araliaceae) [J]. Chin J Nat Med, 2021, 19(9): 648-55.

[13] COSENS D J, MANNING A. Abnormal electroretinogram from a Drosophila mutant [J]. Nature, 1969, 224(5216): 285-7.

[14] MONTELL C, BIRNBAUMER L, FLOCKERZI V, et al. A unified nomenclature for the superfamily of TRP cation channels [J]. Mol Cell, 2002,

9(2): 229-31.
[15] SCHÄFER S, FERIOLI S, HOFMANN T, et al. Mibefradil represents a new class of benzimidazole TRPM7 channel agonists [J]. Pflugers Arch, 2016, 468(4): 623-34.
[16] CHUBANOV V, KÖTTGEN M, TOUYZ R M, et al. TRPM channels in health and disease [J]. Nat Rev Nephrol, 2024, 20(3): 175-87.
[17] DVORNIKOVA K A, PLATONOVA O N, BYSTROVA E Y. The Role of TRP Channels in Colitis and Inflammatory Bowel Disease: A Systematic Review [J]. Int J Mol Sci, 2025, 26(19).
[18] AARTS M, IIHARA K, WEI W L, et al. A key role for TRPM7 channels in anoxic neuronal death [J]. Cell, 2003, 115(7): 863-77.
[19] LIAO X, TANG M, LI J, et al. Acid-Triggered Cascaded Responsive Supramolecular Peptide Alleviates Myocardial Ischemia–Reperfusion Injury by Restoring Redox Homeostasis and Protecting Mitochondrial Function [J]. Adv Healthc Mater, 2025, 14(7): e2404319.
[20] CHEN L, GENG N, CHEN T, et al. Ginsenoside Rb1 Improves Post-Cardiac Arrest Myocardial Stunning and Cerebral Outcomes by Regulating the Keap1/Nrf2 Pathway [J]. Int J Mol Sci, 2023, 24(5).
[21] ZHONG G, CHEN J, LI Y, et al. Ginsenoside Rg3 attenuates myocardial ischemia/reperfusion-induced ferroptosis via the keap1/Nrf2/GPX4 signaling pathway [J]. BMC Complement Med Ther, 2024, 24(1): 247.
[22] GALVAN-ALVAREZ V, GALLEGO-SELLES A, MARTINEZ-CANTON M, et al. Antioxidant enzymes and Nrf2/Keap1 in human skeletal muscle: Influence of age, sex, adiposity and aerobic fitness [J]. Free Radic Biol Med, 2023, 209(Pt 2): 282-91.
[23] WANG Y M, GONG F C, QI X, et al. Mucin 1 Inhibits Ferroptosis and Sensitizes Vitamin E to Alleviate Sepsis-Induced Acute Lung Injury through GSK3β/Keap1-Nrf2-GPX4 Pathway [J]. Oxid Med Cell Longev, 2022, 2022: 2405943.
[24] TSURUSAKI S, KIZANA E. Mechanisms and Therapeutic Potential of Multiple Forms of Cell Death in Myocardial Ischemia-Reperfusion Injury [J]. Int J Mol Sci, 2024, 25(24).
[25] XUAN X, FAN J, ZHANG J, et al. Targeting Programmed Cell Death in Myocardial Ischemia-Reperfusion Injury: Potential Mechanisms and Natural Medicine Treatments [J]. Phytother Res, 2026.
[26] CHEN Z, WU J, LI S, et al. Inhibition of Myocardial Cell Apoptosis Is Important Mechanism for Ginsenoside in the Limitation of Myocardial Ischemia/Reperfusion Injury [J]. Front Pharmacol, 2022, 13: 806216.
[27] XU Z, MENG F, YANG H, et al. BAK and BAX: Therapeutic Targets for Acute Myocardial Infarction and Myocardial Ischemia-Reperfusion Injury [J]. Biology (Basel), 2025, 15(1).
[28] ZHANG Z, CHEN Z, ZHANG S, et al. Antibacterial activity of the structurally novel ocotillol-type lactone and its analogues [J]. Fitoterapia, 2020, 144: 104597.

[29] ZHANG Z, ZENG X, ZHANG S, et al. Novel ocotillol-derived lactone derivatives: design, synthesis, bioactive evaluation, SARs and preliminary antibacterial mechanism [J]. Mol Divers, 2022, 26(4): 2103-20.
[30] STRØBAEK D, HOUGAARD C, JOHANSEN T H, et al. Inhibitory gating modulation of small conductance Ca2+-activated K+ channels by the synthetic compound (R)-N-(benzimidazol-2-yl)-1,2,3,4-tetrahydro-1-naphtylamine (NS8593) reduces afterhyperpolarizing current in hippocampal CA1 neurons [J]. Mol Pharmacol, 2006, 70(5): 1771-82.
[31] SKIBSBYE L, DINESS J G, SØRENSEN U S, et al. The duration of pacing-induced atrial fibrillation is reduced in vivo by inhibition of small conductance Ca(2+)-activated K(+) channels [J]. J Cardiovasc Pharmacol, 2011, 57(6): 672-81.
[32] LI L, WANG Y, GUO R, et al. Ginsenoside Rg3-loaded, reactive oxygen species-responsive polymeric nanoparticles for alleviating myocardial ischemia-reperfusion injury [J]. J Control Release, 2020, 317: 259-72.
[33] DUAN Z, YUAN B, LI H, et al. Ginsenoside Rh2 Exerts a Therapeutic Effect against Myocardial Infarction via Promoting Angiogenesis and Mitochondrial Bioenergetics [J]. J Agric Food Chem, 2025, 73(24): 15056-66.
[34] LI Y, CHEN Y, YU P, et al. Mild therapeutic hypothermic protection activates the PI3K/AKT signaling pathway to inhibit TRPM7 and suppress ferroptosis induced by myocardial ischemia-reperfusion injury [J]. Mol Med Rep, 2024, 30(6).
[35] HU S, LIU G, XIANG H, et al. Myocardial ischemia/reperfusion-induced glycolysis enhances damage through TRPM7 histone lactylation [J]. Toxicol Appl Pharmacol, 2025, 504: 117508.
[36] DENG H, CUI M, LIU L, et al. CIRC-MARC2 SILENCING PROTECTS HUMAN CARDIOMYOCYTES FROM HYPOXIA/REOXYGENATION-INDUCED INJURY BY MODULATING MIR-335-5P/TRPM7 AXIS [J]. Shock, 2024, 61(5): 675-84.
[37] CHUBANOV V, MEDEROS Y SCHNITZLER M, MEISSNE M, et al. Natural and synthetic modulators of SK (K(ca)2) potassium channels inhibit magnesium-dependent activity of the kinase-coupled cation channel TRPM7 [J]. Br J Pharmacol, 2012, 166(4): 1357-76.
[38] PALABIYIK A A. The role of Bcl-2 in controlling the transition between autophagy and apoptosis (Review) [J]. Mol Med Rep, 2025, 32(1).
[39] MA A, ZHU S, YAO X, et al. Ginsenoside Rg3 inhibits melanoma progression by inducing ferroptosis via the p53/SLC7A11/GPX4 pathway [J]. J Adv Res, 2025.
[40] WANG W, WANG F. Ginsenoside Rg3 alleviates allergic rhinitis by regulating NLRP3-mediated inflammatory response and pyroptosis through SIRT6 [J]. Tissue Cell, 2026, 98: 103153.
[41] REN B, FENG J, YANG N, et al. Ginsenoside Rg3 attenuates angiotensin II-induced myocardial hypertrophy through repressing NLRP3 inflammasome and oxidative stress via modulating SIRT1/NF-κB pathway [J]. Int

Immunopharmacol, 2021, 98: 107841.

Supplementary Files

This is a list of supplementary files associated with this preprint. Click to download.

- uncroppedblotsimages.pdf